

Magnetic Internal Compton Coefficients in the Born Approximation*

LARRY SPRUCH AND G. GOERTZEL

Physics Department, Washington Square College, New York University, New York, New York

(Received March 15, 1954)

The absolute and relative probabilities of a nuclear transition in which there is a simultaneous ejection of a K electron and emission of a gamma ray has been calculated quantum-mechanically for the case in which the virtual radiation field is a 2^L magnetic multipole. The process will be referred to as an internal Compton effect. The Born approximation has been used and hence the calculations are expected to be valid only if the nuclear charge Z is small and the nuclear energy level separation large. The ratio of the number of continuous energy gamma rays to the number of discrete energy K electrons is independent of the nuclear matrix element and *decreases* as Z or as L increases. This is true for any energy range and any angular range of the continuous energy gamma rays, where the angles are measured with respect to the coincident continuous energy K electron. The angular distribution is most sensitive to L for comparable electron and gamma-ray energies and for large angular separation. These conclusions are not much affected by inclusion of the L shell. In the limit of small gamma-ray energies, the results reduce to those predicted by semiclassical theory.

I. INTRODUCTION

THE transition of a nucleus to a lower state of the same nucleus by the emission of a gamma ray or by the ejection of an orbital electron, i.e., internal conversion, is very well known. Another possible mode of decay is the simultaneous emission of a gamma ray and ejection of an orbital electron; the electron and the nucleus exchange a virtual photon and the electron emits a real gamma ray. This process bears the same relationship to the Compton effect as internal pair production does to pair production, and will be referred to as the internal Compton effect. In the same sense, internal conversion is often referred to as the internal photoeffect. In all of these cases, the essential distinction between the internal and the external process is the presence of a virtual rather than a real photon.

The relative probability of the internal Compton effect is quite small and thus far the effect has been detected¹ only in the case of Ba^{137m} .² One should, nevertheless, have some quantitative estimate of its probability if only in order to be able to correct for the contributions due to this event in measurements of the internal conversion coefficient, or the angular correlation between a gamma ray and a beta particle emitted in cascade, or the angular correlation between a gamma ray and an internally converted electron emitted in cascade. In these latter cases the distinction between the process under consideration and the internal Compton effect can also be made by energy measurements, but this is often quite difficult.

The probability of an internal Compton transition was considered previously by Cooper and Morrison³

* One of the authors (L.S.) was partially supported by the U. S. Atomic Energy Commission.

¹ H. B. Brown and R. Stump, *Phys. Rev.* **90**, 1061 (1953).

² The present calculation cannot be expected to be valid for this nucleus. See L. Spruch and G. Goertzel, *Phys. Rev.* **93**, 642 (1954).

³ E. P. Cooper and P. Morrison, *Phys. Rev.* **57**, 862 (1940). We would like to thank Dr. J. Levinger for calling our attention to this article.

who refer to the process as internal scattering. The calculation was limited to high-energy electric dipole transitions and is not valid over the entire range of permissible electron energies. Angular correlation between the electron and the photon was not considered.

A similar process, inner bremsstrahlung, i.e., photon production accompanying charged particle transformations, has been studied in the past in connection with nuclear β decay,^{4,5} K capture,^{6,7} charged meson production in high-energy nuclear collisions,^{8,9} the decay of charged π mesons,^{10,11} and μ decay.^{12,13}

II. NOTATION

ψ_{N_0} , ψ_{N_f} , ψ_0 , and ψ_f are the initial and final nuclear and electronic wave functions, respectively.

(p_0, \mathbf{p}) , (E, \mathbf{P}) , (q, \mathbf{q}) , and (k_0, \mathbf{k}) are the energy-momentum four-vectors of the electron in the intermediate state, the electron in the final state, the real photon, and the virtual photon, respectively.

E_0 = energy of the electron in the ground state.

W = energy given up by the nucleus.

ΔE and $\Delta E_K(e+\gamma)$ are the total width and the K shell internal Compton width, respectively, of the initial nuclear energy level.

$\mathbf{Q} = \mathbf{P} + \mathbf{q}$.

θ is the angle between \mathbf{P} and \mathbf{q} .

$\mu = \cos\theta$.

$E' = E - P\mu$.

⁴ J. K. Knipp and G. E. Uhlenbeck, *Physica* **3**, 425 (1936); F. Bloch, *Phys. Rev.* **50**, 272 (1936).

⁵ C. S. W. Chang and D. L. Falkoff, *Phys. Rev.* **76**, 365 (1949).

^{6a} Madansky, Lipps, Bolgiano, and Berlin, *Phys. Rev.* **84**, 596 (1951).

⁶ P. Morrison and L. I. Schiff, *Phys. Rev.* **58**, 24 (1940).

⁷ J. M. Jauch, Oak Ridge National Laboratory Report ORNL-1102, 1951 (unpublished).

⁸ S. Mayakawa and S. Tomonaga, *Progr. Theoret. Phys. (Japan)* **2**, 161 (1947).

⁹ L. I. Schiff, *Phys. Rev.* **76**, 89 (1949).

¹⁰ H. Primakoff, *Phys. Rev.* **84**, 1255 (1951).

¹¹ T. Eguchi, *Phys. Rev.* **85**, 943 (1952).

¹² D. B. Feer, *Phys. Rev.* **75**, 731 (1949).

¹³ A. Lenard, *Phys. Rev.* **90**, 968 (1953).

α = fine structure constant.

Z = nuclear charge.

$\mathfrak{F} = [(Q^2 - W^2)^2 + (2mW\alpha Z)^2]^{-1}$.

K_+^* , K_+ , and δ_+ are the propagation kernels of an electron in a potential V , a free electron, and a photon, respectively.

$$K_+(\mathfrak{x}_7, \mathfrak{x}_5) = (i/16\pi^4) \int (\mathfrak{p} - m)^{-1} \exp(-i\mathfrak{p} \cdot \mathfrak{x}_7) d^3\mathfrak{p} d p_0$$

$$\delta_+[(\mathfrak{x}_6 - \mathfrak{x}_5)^2] = -(1/4\pi^3) \int \exp(-i\mathfrak{f} \cdot \mathfrak{x}_{65}) \mathfrak{f}^{-2} d^3\mathfrak{k} d k_0.$$

M_1 and M_2 are the matrix elements corresponding to the two possible Feynman diagrams for an internal Compton transition.

J_0 , m_0 , J_f , m_f , and L , M are the angular momentum quantum numbers of the initial and final nuclear states and of the virtual radiation field, respectively.

$\mathbf{A}_{LM}^{(m)}$ and $\mathbf{B}_{LM}^{(m)}$ are the magnetic vector potentials of the radiation field multipoles which interact with the nucleus and electron, respectively.

$M_N(L, m_0, m_f, M)$ is a nuclear matrix element.

$|M_N(L)|^2$ is proportional to a sum of squares of nuclear matrix elements.

$$\mathbf{I} = \int \exp(-i\mathbf{Q} \cdot \mathbf{x}) \mathbf{B}_{LM}^{(m)}(W\mathbf{x}) e^{-m\alpha Z x} d^3\mathbf{x}.$$

$(\mathbf{F}; \mathbf{G}) = 2(\mathbf{F} \cdot \mathbf{I})(\mathbf{G} \cdot \mathbf{I})$, for arbitrary F and G .

R_L is a radial integral.

K and L refer to the respective shells.

\mathcal{P}_K is the absolute probability of an internal Compton transition.

$R_K(L; q_1, q_2; \theta)$ and $R_K(L; q_1, q_2)$ are magnetic internal Compton transition rates.

$B_K(L; q_1, q_2; \theta)$ and $B_K(L; q_1, q_2)$ are magnetic internal Compton coefficients.

$\mathcal{R}_K(L)$ is a magnetic internal conversion rate.

$\beta_K(L)$ is a magnetic internal conversion coefficient.

$[\mathbf{n}] = (\mathbf{n}_1, \mathbf{n}_2, \mathbf{n}_3)$ represents a set of unit vectors fixed in space.

III. MATRIX ELEMENTS

We take as our initial state one in which the nucleus is in an excited state with angular momentum J_0 and the K shell is filled. We want to find the absolute and relative probabilities that after some time the nucleus is in a lower energy state with angular momentum J_f and that either K electron has been ejected and a coincident gamma ray has been emitted. We also want to find the energy distribution of these gamma rays and their angular correlation with respect to the electrons. It will be assumed that in the absence of orbital electrons the gamma ray emitted in the transition is a pure 2^L magnetic multipole. The angular momentum projections of the initial and final nuclear states, m_0 and

m_f , and the projection of the spin of the electron, are defined with respect to the axis \mathbf{n}_3 of the set of unit vectors $\mathbf{n}_1, \mathbf{n}_2, \mathbf{n}_3$ fixed in space and denoted by $[\mathbf{n}]$.

The probability \mathcal{P}_K that at some much later time this internal Compton process will have taken place is given by

$$\mathcal{P}_K = \int \mathcal{S} |M_1 + M_2|^2 (2\pi)^{-6} P E d E q^2 d q d \omega_e d \omega_\gamma, \quad (1)$$

where

$$\mathcal{S} = (2J_0 + 1)^{-1} \sum_{m_0} \sum_{m_f} \sum_{S_0} \sum_{S_f} S_{S_0} S_{S_f}. \quad (2)$$

\mathcal{S} represents the average over the initial state and the sum over the final state angular momentum projections of the nucleus, the sum over the initial and the final electron spin projections, and the sum over the states of polarization of the gamma ray. The matrix elements M_1 and M_2 follow immediately¹⁴ from the Feynman diagrams 1 and 2 drawn in Fig. 1.

M_1 is given by

$$M_1 = -e^2 \int \bar{\psi}_{N_f}(\mathfrak{x}_6) \bar{\psi}_f(\mathfrak{x}_7) \mathbf{A}(\mathfrak{x}_7) K_+^v(\mathfrak{x}_7, \mathfrak{x}_5) \gamma_{N\mu} \gamma_\mu \times \delta_+[(\mathfrak{x}_6 - \mathfrak{x}_5)^2] \psi_{N_0}(\mathfrak{x}_6) \psi_0(\mathfrak{x}_5) d^4\mathfrak{x}_5 d^4\mathfrak{x}_6 d^4\mathfrak{x}_7, \quad (3)$$

where

$$\mathbf{A}(\mathfrak{x}_7) = \gamma_\nu S_\nu e^{2\pi/q} e^{-i(\mathbf{q} \cdot \mathfrak{x}_7 - q t_7)}. \quad (4)$$

The S_ν represent the states of polarization of the real photon. We substitute in the explicit expressions for δ_+ and use the relationships

$$\int d k_0 e^{-i k_0 t_{65}} \int \frac{e^{i\mathbf{k} \cdot (\mathbf{x}_6 - \mathbf{x}_5)}}{k_0^2 - \mathbf{k} \cdot \mathbf{k}} d^3\mathbf{k} = -2\pi^2 \int \frac{e^{i|k_0| x_{65}}}{x_{65}} e^{-i k_0 t_{65}} d k_0, \quad (5)$$

where $x_{65} = |\mathbf{x}_6 - \mathbf{x}_5|$, and $\gamma_{N\mu} \gamma_\mu = \beta_N \beta (1 - \alpha_N \cdot \alpha)$. By our assumption as to the nature of the nuclear states,

$$(1 - \alpha_N \cdot \alpha) e^{i|k_0| x_{65}} (x_{65})^{-1} \quad (6)$$

can be replaced by that portion of it which is proportional to the interactions of the nucleus and of the

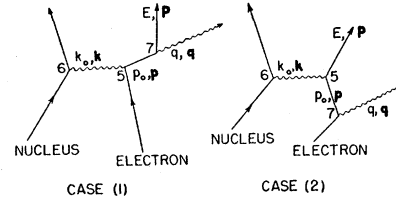


FIG. 1. Feynman diagrams for an internal Compton transition.

¹⁴ We follow rather closely the methods and notation of Feynman, with some slight notational modifications as introduced by Baranger, Bethe, and Feynman. We use the normalization $u^\dagger u = 1$. R. P. Feynman, Phys. Rev. **76**, 749, 769 (1949); Baranger, Bethe, and Feynman, Phys. Rev. **92**, 482 (1953), see in particular reference 8.

electron with a magnetic $2L$ pole, that is, by¹⁵

$$2\pi^2 i |k_0|^{-1} [\boldsymbol{\alpha}_N \cdot \mathbf{A}_{LM}^{*(m)}(|k_0| \mathbf{x}_6)] \times [\boldsymbol{\alpha} \cdot \mathbf{B}_{LM}^{(m)}(|k_0| \mathbf{x}_6)], \quad (7)$$

where

$$M = m_0 - m_f,$$

$$\mathbf{A}_{LM}^{(m)}(|k_0| \mathbf{x}_6) = N j_L(|k_0| x_6) i \mathbf{L} Y_{LM}(\mathbf{x}_6, [\mathbf{n}]), \quad (8)$$

$$\mathbf{B}_{LM}^{(m)}(|k_0| \mathbf{x}_6) = N h_L^{(1)}(|k_0| x_6) i \mathbf{L} Y_{LM}(\mathbf{x}_6, [\mathbf{n}]), \quad (9)$$

$$N = \{2/[\pi L(L+1)]\}^{\frac{1}{2}} |k_0|.$$

$Y_{LM}(\mathbf{x}, [\mathbf{n}])$ is a spherical harmonic whose polar angles are those of the vector \mathbf{x} with respect to the set of fixed axes $[\mathbf{n}]$. The spherical Bessel function, j_L , and the spherical Hankel function of the first kind, $h_L^{(1)}$, are defined as in Schiff.¹⁶ In the above replacement, the quite negligible contribution due to those cases in which the orbital electron is ejected from within the nucleus has been ignored.

Since the initial state of the nucleus has a width ΔE (which is proportional to its initial rate of decay by any process whatever), we can write (see Appendix III)

$$\int_0^\infty e^{it_6(-k_0 - W + i\Delta E)} dt_6 = i f', \quad (10)$$

where

$$f' = (-k_0 - W + i\Delta E)^{-1}. \quad (11)$$

We now have

$$M_1 = \pi e^2 \int M_N'(L, m_0, m_f, M) |k_0|^{-1} \bar{\psi}_f(\boldsymbol{\xi}_7) A(\boldsymbol{\xi}_7) \times K_+^v(\boldsymbol{\xi}_7, \boldsymbol{\xi}_5) \beta \boldsymbol{\alpha} \cdot \mathbf{B}_{LM}^{(m)}(|k_0| \mathbf{x}_6) e^{+ik_0 t_6} \times \psi_0(\boldsymbol{\xi}_5) f' d^4 \boldsymbol{\xi}_5 d^4 \boldsymbol{\xi}_7 d\mathbf{k}_0, \quad (12)$$

where we have defined a nuclear matrix element,

$$M_N'(L, m_0, m_f, M) = \int \bar{\psi}_{Nf}(\mathbf{x}_6) \beta_N \boldsymbol{\alpha}_N \cdot \mathbf{A}_{LM}^{*(m)}(|k_0| \mathbf{x}_6) \times \psi_{N0}(\mathbf{x}_6) d^3 \mathbf{x}_6. \quad (13)$$

At this point we make a number of approximations which should be valid when the nuclear charge is small, and when the energy given up by the nucleus, W , is of the order of or larger than m .

(1) It is assumed that the electron in the intermediate state is free, i.e., K_+^v is replaced by K_+ .

(2) It is assumed that the electron in the final state is free, i.e.,

$$\bar{\psi}_f(\boldsymbol{\xi}_7) = \bar{\psi}_f(\mathbf{x}_7) e^{-iE t_7} \rightarrow u_f e^{-i(\mathbf{P} \cdot \mathbf{x}_7 - E t_7)}, \quad (14)$$

where $P = (E^2 - m^2)^{\frac{1}{2}}$.

¹⁵ N. Trall and G. Goertzel, Phys. Rev. **83**, 399 (1951). See Appendix A.

¹⁶ L. I. Schiff, *Quantum Mechanics* (McGraw-Hill Book Company, Inc., New York, 1949).

(3) The small components of the electron ground state are neglected and the Dirac large components are replaced by the Schrödinger components, i.e.,

$$\psi_0(\boldsymbol{\xi}_5) = \psi_0(\mathbf{x}_5) e^{-iE_0 t_5} \rightarrow \pi^{-\frac{1}{2}} (m\alpha Z)^{\frac{1}{2}} e^{-m\alpha Z x_5 - iE_0 t_5} u_0, \quad (15)$$

where

$$u_0^\dagger = (1, 0, 0, 0) \quad \text{or} \quad (0, 1, 0, 0). \quad (16)$$

The neglect of the small components, unlike the first two approximations, does not greatly simplify the calculation. It is done since it is consistent with these approximations, where terms in αZ have already been neglected. The replacement of Dirac large components by Schrödinger components gives rise to an error of order $(\alpha Z)^2$.

(4) The binding energy of the electron in the ground state, which is of course proportional to $m(\alpha Z)^2$, is neglected with respect to its rest energy, i.e., E_0 is replaced by m .

With these approximations it is a trivial matter to carry through the integrations over t_7 , t_5 , k_0 , p_0 , \mathbf{x}_7 , and \mathbf{p} , in the given order. We then find

$$M_1 = i\pi^2 e^3 2^{\frac{1}{2}} (m\alpha Z)^{\frac{1}{2}} (q^{\frac{1}{2}} W)^{-1} f M_N(L, m_0, m_f, M) (E')^{-1} T_1, \quad (17)$$

where

$$T_1 = (u_f^\dagger \boldsymbol{\alpha} \cdot \mathbf{S} [W + \boldsymbol{\alpha} \cdot \mathbf{Q}] \boldsymbol{\alpha} \cdot \mathbf{I} u_0), \quad (18)$$

$$\mathbf{Q} = \mathbf{P} + \mathbf{q}, \quad (19)$$

$$\mathbf{I} = \int \exp(-i\mathbf{Q} \cdot \mathbf{x}) \mathbf{B}_{LM}^{(m)}(W\mathbf{x}) e^{-m\alpha Z x} d^3 \mathbf{x}, \quad (20)$$

$$E' = E - P\mu, \quad (21)$$

$$f = (-W - m + E + q + i\Delta E)^{-1} \quad (22)$$

$$M_N(L, m_0, m_f, M) = \int \bar{\psi}_{Nf}(\mathbf{x}_6) \beta_N \boldsymbol{\alpha}_N \cdot \mathbf{A}_{LM}^{*(m)}(W\mathbf{x}_6) \psi_{N0}(\mathbf{x}_6) d^3 \mathbf{x}_6. \quad (23)$$

In arriving at the above result, we have made use of the fact that $\gamma_\nu S_\nu$ represents a real photon so that

$$\gamma_\nu S_\nu = \beta \boldsymbol{\alpha} \cdot \mathbf{S},$$

we have used $\beta u_0 = u_0$, and we have dropped the subscript 5 on \mathbf{x}_6 in the expression for \mathbf{I} . We have further replaced $(E + q - m)$ by W in all terms other than f , which is permissible due to the form of f , as we shall see later.

Proceeding in the same manner, but making the further approximation that Fourier momentum components of the ground state of order m can be neglected (see Appendix IV), we find for M_2

$$M_2 = i\pi^2 e^3 2^{\frac{1}{2}} (m\alpha Z)^{\frac{1}{2}} (q^{\frac{1}{2}} W)^{-1} f M_N(L, m_0, m_f, M) m^{-1} T_2, \quad (24)$$

where

$$T_2 = (u_f^\dagger \boldsymbol{\alpha} \cdot \mathbf{I} [q + \boldsymbol{\alpha} \cdot \mathbf{q}] \boldsymbol{\alpha} \cdot \mathbf{S} u_0). \quad (25)$$

Performing sums in the usual way, we find

$$S_0 S_f S_{\nu} |M_1 + M_2|^2 = \frac{8\pi^4 e^6 (m\alpha Z)^3 |M_N(L, m_0, m_f, M)|^2 |f|^2}{q^3 W^2 E} H, \quad (26)$$

where

$$H = (E')^{-2} |\mathbf{I}|^2 [q^2 E' + W P^2 (1 - \mu^2)] + (mE')^{-1} [|\mathbf{I}|^2 q P^2 (\mu^2 - 1) - m(\mathbf{q}; \mathbf{q}) + q(\mathbf{P}; \mathbf{P}) - P\mu \operatorname{Re}(\mathbf{P}; \mathbf{q})] + (q/m^2) [|\mathbf{I}|^2 q E + \operatorname{Re}(\mathbf{P}; \mathbf{q})], \quad (27)$$

where Re denotes the real part, and where, for arbitrary vectors \mathbf{F} and \mathbf{G} ,

$$(\mathbf{F}; \mathbf{G}) = 2(\mathbf{F} \cdot \mathbf{I})(\mathbf{G} \cdot \mathbf{I}). \quad (28)$$

In the above expressions, the M in $M_N(L, m_0, m_f, M)$ and in the expressions of the form $(\mathbf{F}; \mathbf{G})$ represents $m_0 - m_f$. It is permissible, however, to consider M arbitrary and to sum over M , for only the one value $m_0 - m_f$ will contribute. If we now define $|M_N(L)|^2$ by the relation

$$(2J_0 + 1)^{-1} \sum_{m_0} \sum_{m_f} |M_N(L, m_0, m_f, M)|^2 = |M_N(L)|^2, \quad (29)$$

$|M_N(L)|^2$ is independent of M and we obtain

$$\mathcal{O}_K = \frac{e^6 (m\alpha Z)^3 |M_N(L)|^2}{8\pi^2 W^2} \times \int q^{-1} |f|^2 P(\sum_M H) dE d\omega d\omega_\gamma. \quad (30)$$

IV. RESULTS

It can be seen from the results derived in the appendices that the only angular dependence of the integrand of \mathcal{O}_K is the dependence upon μ . The angular integrations thus reduce to

$$\int \cdots d\omega d\omega_\gamma = (4\pi)(2\pi) \int_{-1}^1 \cdots d\mu. \quad (31)$$

Further, for any slowly varying function of E , $g(E)$, we have, ignoring terms in $(\Delta E)/(W - q)$,

$$\begin{aligned} & \int_m^\infty g(E) |f|^2 dE \\ &= \int_m^\infty g(E) [(-W - m + E + q)^2 + (\Delta E)^2]^{-1} dE \\ &= g(W + m - q) \pi (\Delta E)^{-1}. \end{aligned} \quad (32)$$

\mathcal{O}_K can now be expressed in the form $\Delta E_K(e + \gamma)/\Delta E$, where $\Delta E_K(e + \gamma)$ is that part of the width of the initial state which is due to the probability of decay via a K -shell internal Compton transition. Since an initial transition rate is given by twice the corresponding width, the initial transition rate for an internal Compton

process in which the gamma ray has an energy between q_1 and q_2 and in which either K electron has been ejected is given by

$$R_K(L; q_1, q_2) = 16\pi e^6 (m\alpha Z)^3 |M_N(L)|^2 (2L + 1) \times \int_{q_1}^{q_2} dq \int_{-1}^1 d\mu q^{-1} P |R_{LL}|^2 \mathfrak{C}, \quad (33)$$

where

$$\begin{aligned} \mathfrak{C} &= (E')^{-2} [W P^2 (1 - \mu^2) + q^2 E'] \\ &\quad - (mE')^{-1} [q P^2 (1 - \mu^2) (mq + P^2 + Pq\mu) Q^{-2}] \\ &\quad + (q/m^2) [q E' - P^2 q^2 (1 - \mu^2) Q^{-2}], \end{aligned} \quad (34)$$

$$E = W + m - q, \quad (35)$$

$$|R_L|^2 = (1/W^2) (Q^2/W^2)^L \mathfrak{F}, \quad (36)$$

$$\mathfrak{F} = [(Q^2 - W^2)^2 + (2mW\alpha Z)^2]^{-1}. \quad (37)$$

Use has been made of the results derived in the appendices. As in the notation for internal conversion, the dependence of the rate upon W and Z has been suppressed. A transition rate $R_K(L; q_1, q_2; \theta)$ per unit solid angle for an angle θ between the electron and the gamma ray can also be defined.

While in principle measurements can be made in which the lower limit q_1 approaches zero, the calculated rate diverges in this limit. There is no need, however, to modify the calculations so as to properly eliminate this infrared catastrophe, for experimentally it would be difficult to distinguish a very low-energy internal Compton gamma ray in coincidence with a continuous energy electron from an x-ray of comparable energy in coincidence with an "ordinary" internally converted electron with the maximum possible energy. The experimental procedure would then be to measure only those gamma rays above some minimum energy q_1 , which is above the maximum x-ray energy for the given nucleus. It is to be noted that in a calculation of the energy imparted to the continuous gamma rays, the extra factor of q in the integrand automatically eliminates the infrared catastrophe. This energy calculation would probably be fairly accurate even though the number of very low-energy gamma rays is of course incorrectly given.

While the upper limits q_2 can be set equal to the true maximum W without any divergence, the calculations are not valid in this energy region for the electron energy is then so small that the Born approximation cannot be used.

To the same Born approximation, the transition rate for the internal conversion of either K electron is given by¹⁷

$$\mathcal{O}_K(L) = 8\pi^2 e^4 m (\alpha Z)^3 (2L + 1) \times |M_N(L)|^2 (W + 2m)^{L + \frac{1}{2}} (W)^{-L - 5/2}. \quad (38)$$

¹⁷ S. M. Dancoff and P. Morrison, Phys. Rev. 55, 122 (1939).

The coefficient of $|M_N(L)|^2$ is of course known exactly,¹⁸ but the calculation of the probability of an internal Compton process relative to that of an internal conversion process will probably be more reliable if the inexact $\mathcal{R}_K(L)$ is used, for it then involves approximations quite similar to those used in the evaluation of $R_K(L; q_1, q_2)$ and $R_K(L; q_1, q_2; \theta)$. In any event, the calculated relative probability will only be reliable in those regions for which the difference between the Born approximation and exact internal conversion rate is not too great.

The ratios,

$$B_K(L; q_1, q_2) = R_K(L; q_1, q_2) / \mathcal{R}_K(L), \quad (39)$$

and

$$B_K(L; q_1, q_2; \theta) = R_K(L; q_1, q_2; \theta) / \mathcal{R}_K(L), \quad (40)$$

will be referred to as the total and differential magnetic K -shell internal Compton coefficients, respectively, for a multipole of order L . The latter coefficient, for example, represents the ratio of the number of gamma rays emitted with energies between q_1 and q_2 per unit solid angle at an angle θ with respect to the coincident K electron to the number of discrete energy K electrons in the case of a 2^L magnetic multipole. The letter B is chosen in analogy with the magnetic internal conversion coefficient β . From their definitions, it follows that

$$B_K(L; q_1, q_2; \theta)$$

$$= \frac{e^2 m^2}{\pi^2 W L^{-\frac{1}{2}} (W + 2m)^{L+\frac{1}{2}}} \int_{q_1}^{q_2} dq \frac{P}{q} Q^{2L} \mathcal{C} \mathcal{F}, \quad (41)$$

and

$$B_K(L; q_1, q_2) = 2\pi \int_{-1}^1 B_K(L; q_1, q_2; \theta) d\mu. \quad (42)$$

The corresponding quantities for the L shell follow immediately if, as is consistent with our previous approximations, we neglect the $2p$ contribution and the small components of the $2s$ electrons, and approximate the spatial dependence of the large components by the Schrödinger components with terms proportional to αZ neglected, in which case

$$\psi_{2s}(x, Z) = \psi_{1s}(x, Z/2). \quad (43)$$

The L -shell coefficients therefore follow from the K -shell coefficients by the replacement of Z by $(Z/2)$. However, $B_K(L; q_1, q_2; \theta)$ is roughly independent of Z except in the neighborhood of $Q=W$ where the dependence of \mathcal{F} upon Z is essential. If this region is then not included in the measurement, it follows, since

$$\beta_K(L) \approx 8\beta_L(L), \quad (44)$$

that

$$B_{K+L}(L; q_1, q_2; \theta) \approx (8/9)B_K(L; q_1, q_2; \theta) + (1/9)B_L(L; q_1, q_2; \theta) \approx B_K(L; q_1, q_2; \theta). \quad (45)$$

¹⁸ Rose, Goertzel, Spinrad, Harr, and Strong, Phys. Rev. **76**, 1883 (1949).

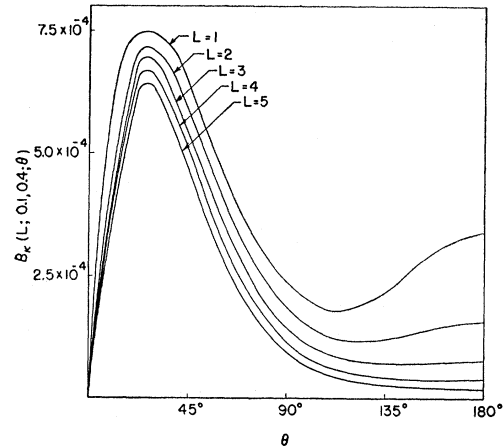


Fig. 2. $B_K(L; 0.1, 0.4; \theta)$ is the ratio of the number of gamma rays emitted per unit solid angle with energies between $0.1 mc^2$ and $0.4 mc^2$ to the number of discrete energy K electrons. The nucleus, of charge $Z=20$, makes a transition corresponding to a 2^L magnetic multipole of energy $1.29 mc^2$. θ is the angle between the photon and the coincident K electron.

Although the L -shell maximum is four times that of the K shell, the factor $(1/9)$ and the occurrence of the maxima in the same region cause this last relation to be approximately valid even when the region $Q=W$ is included. Obviously, to the same degree of validity, there exists the similar relation

$$B_{K+L}(L; q_1, q_2) \approx B_K(L; q_1, q_2).$$

The expression for $B_K(L; 0.1, 0.4; \theta)$ has been integrated numerically for one set of values of Z , W , q_1 and q_2 . The results are shown in Fig. 2. The effect of a change in Z for these energies can be seen by a comparison with the results previously reported for Ba^{137m} .² For $\theta=0^\circ$ or 180° \mathcal{C} reduces to the very simple form

$$\mathcal{C}(\theta=0^\circ \text{ or } 180^\circ) = 2Eq^2/m^2. \quad (46)$$

The $B_K(L; q_1, q_2; \theta)$ can then be readily calculated for these angles.

As $q \rightarrow 0$, it is found that

$$B_K(L; q, q + dq; \theta) \rightarrow \frac{e^2 \beta^2 (1 - \mu^2) dq}{4\pi^2 (1 - \beta\mu)^2 q}, \quad (47)$$

where

$$\beta = P/E.$$

This is precisely the result derived semiclassically by Wang Chang and Falkoff¹⁹ for the case of the inner bremsstrahlung associated with β decay, where it was shown to arise from the instantaneous acceleration of the electron. The relationship also follows quite generally,²⁰ in the limit as αZ and the photon energy approach zero, on comparing the squared matrix element for an arbitrary graph with one obtained from it by

¹⁹ See reference 5. Note that our coefficient is defined per unit solid angle.

²⁰ See reference 13 and R. Jost, Phys. Rev. **72**, 815 (1947).

inserting into an external spinor line an external photon line.

V. DISCUSSION

Ignoring any small trends in $|M_N(L)|^2$ with increasing Z , the Z dependence of the internal Compton transition rate is contained in the factors Z^3 and \mathfrak{F} . If the measurements do not include the region $Q \approx W$, the Z dependence of \mathfrak{F} can be neglected and the rate exhibits a Z^3 dependence. If they include only the region $Q \approx W$, \mathfrak{F} has a maximum at $Q=W$ which shows a $(1/Z^2)$ dependence while the width of the maximum has a Z dependence; the integral is then proportional to $(1/Z)$ and the rate has a Z^2 dependence. The L dependence of the rate, for those values of L that are allowed by the selection rules, is determined essentially by the strong L dependence of $|M_N(L)|^2$, which decreases sharply with increasing L . This dependence cannot be offset by the factor $(2L+1)(Q^2/W^2)^L$ since for W of the order of or greater than m , for which the calculations are valid, (Q^2/W^2) cannot be more than about 3, the value it assumes for $W=m$, $q \approx 0$.

The Z dependence of the internal Compton coefficients is contained in the factor \mathfrak{F} . Therefore, unlike the internal conversion coefficients, they *decrease* as Z increases. However, $B_K(L; q_1, q_2; \theta)$ will be relatively independent of Z except in the region $Q \approx W$. Their L dependence is contained in the factor

$$[Q^2/(W^2+2Wm)]^L.$$

Since the argument within the square brackets is less than or equal to one, they *decrease* as L increases, again unlike the internal conversion coefficients. The L dependence of $B_K(L; q_1, q_2; \theta)$ will be strongest for large angles θ , due to the factor Q^{2L} . If θ and q_2 are small, $B_K(L; q_1, q_2; \theta)$ will be relatively insensitive to L .

Because the Born approximation was used, the results can be expected to be valid only if $maZ/P \ll 1$. A similar requirement holds for the intermediate states. For the Feynman diagrams 1 and 2, we have $\mathbf{p}=\mathbf{Q}$ and $\mathbf{p}=-\mathbf{q}$, respectively. These relations follow from conservation of momentum at the real photon junction. The calculation of M_1 is valid then only if $maZ/Q \ll 1$; however, if $Q \approx 0$, almost all of the small contribution (the total contribution vanishes at $Q=0$) comes from $|M_2|^2$. This can be seen by an analysis of \mathfrak{F} , whose three terms originate in $|M_1|^2$, the cross term, and $|M_2|^2$, respectively, for, as $Q \rightarrow 0$,

$$\begin{aligned} P \rightarrow W(W+2m) \cdot \frac{1}{2}(m+W)^{-1}, \\ P^2(1-\mu^2)Q^{-2} \rightarrow 1. \end{aligned}$$

Similarly, the calculation of M_2 is valid only if $maZ/q \ll 1$; however, if $q \approx 0$, almost all of the contribution comes from $|M_1|^2$. Another possible criterion is that the calculations will be valid only for those values of Z and W for which the Born approximation calculations of the $\beta_K(L)$ are valid. On the one hand, the $B_K(L; q_1, q_2; \theta)$ can be expected to be more reliable than the $\beta_K(L)$,

since the former involve the ratio of two calculations in which similar approximations have been made. On the other hand, the $B_K(L; q_1, q_2; \theta)$ refer to a more complicated process involving intermediate states which are also treated by the Born approximation.

The ratio of continuous gamma rays to discrete gamma rays is given by

$$B_K(L; q_1, q_2; \theta)\beta_K(L).$$

(This ratio, rather than the one chosen, might well have been called the internal Compton coefficient.) In this case, the exact $\beta_K(L)$ should be used.

Calculations of the electrical internal Compton coefficients are in progress. (See also reference 3.)

We would like to thank Miss Pearl Ehrlich for performing the numerical calculations.

APPENDIX I

Evaluation of $\sum_M |I|^2$ and of $\sum_M (F; G)$

The integral **I** is defined by Eqs. (9) and (20). If we define

$$\begin{aligned} (L\nu | \mathbf{L} | LM) \text{ by } \mathbf{L} Y_{LM}(\mathbf{x}, [\mathbf{n}]) \\ = \sum_{\nu} Y_{L\nu}(\mathbf{x}, [\mathbf{n}]) (L\nu | \mathbf{L} | LM), \end{aligned}$$

and note that

$$\begin{aligned} \exp(-i\mathbf{Q} \cdot \mathbf{x}) \\ = 4\pi \sum_{l,p} (-i)^l j_l(Qx) Y_{lp}(\mathbf{Q}, [\mathbf{n}]) Y_{lp}^*(\mathbf{x}, [\mathbf{n}]), \end{aligned}$$

we may write

$$\mathbf{I} = \{32\pi/[L(L+1)]\}^{\frac{1}{2}} (-i)^{L-1} W R_L \mathbf{L} Y_{LM}(\mathbf{Q}, [\mathbf{n}]),$$

where

$$R_L = \int_0^\infty h_L^{(1)}(Wx) j_L(Qx) e^{-maxx} x^2 dx. \quad (\text{A-1})$$

Consider now the dyadic D defined by

$$D = \sum_M [\mathbf{L} Y_{LM}(\mathbf{Q}, [\mathbf{n}])] [\mathbf{L} Y_{LM}(\mathbf{Q}, [\mathbf{n}])]^*.$$

Since

$$(L\sigma | \mathbf{L} | LM)^* = (LM | \mathbf{L} | L\sigma),$$

and since \mathbf{L} connects only states with the same L , the expression becomes

$$\begin{aligned} D &= \sum_{M, \nu, \sigma} Y_{L\nu}(\mathbf{Q}, [\mathbf{n}]) \\ &\quad \times (L\nu | \mathbf{L} | LM) (LM | \mathbf{L} | L\sigma) Y_{L\sigma}^*(\mathbf{Q}, [\mathbf{n}]) \\ &= \sum_{\nu\sigma} Y_{L\nu}(\mathbf{Q}, [\mathbf{n}]) (L\nu | \mathbf{L} | L\sigma) Y_{L\sigma}^*(\mathbf{Q}, [\mathbf{n}]). \end{aligned}$$

The basis $[\mathbf{n}]$ affects the terms in the sum only in determining the projections ν and σ ; since ν and σ are summed over, D is independent of the basis. It is convenient to choose a basis $[\mathbf{u}] = (\mathbf{u}_1, \mathbf{u}_2, \mathbf{u}_3)$ in which \mathbf{u}_3 is in the direction of \mathbf{Q} . The polar angle is then 0 and D reduces to

$$\begin{aligned} D &= |Y_{L0}(0, \phi)|^2 (L0 | \mathbf{L} | L0) \\ &= (2L+1)/(4\pi) (L0 | \mathbf{L} | L0). \end{aligned}$$

The dyadic is then invariant under a rotation about \mathbf{u}_3

and is symmetric in the first and second unit vectors. It must then be possible to write

$$(L0|\mathbf{LL}|L0) = a(\mathbf{u}_1\mathbf{u}_1 + \mathbf{u}_2\mathbf{u}_2) + b\mathbf{u}_3\mathbf{u}_3.$$

Since

$$L u_3 Y_{L0}(\mathbf{Q}, [\mathbf{u}]) = 0,$$

the coefficient b vanishes. Taking the spur of both sides gives $L(L+1) = 2a$, and thus

$$D = L(L+1)(2L+1)(1/8\pi)(\mathbf{u}_1\mathbf{u}_1 + \mathbf{u}_2\mathbf{u}_2).$$

From the definition of D , it follows that

$$\begin{aligned} \sum_M |\mathbf{I}|^2 &= \{32\pi/[L(L+1)]\} W^2 |R_L|^2 \text{Spur } D \\ &= 8(2L+1)W^2 |R_L|^2, \end{aligned}$$

and that

$$\begin{aligned} \sum_M (\mathbf{F}; \mathbf{G}) &= 2 \sum_M (\mathbf{F} \cdot \mathbf{I})(\mathbf{I} \cdot \mathbf{G}) \\ &= \{64\pi/[L(L+1)]\} W^2 |R_L|^2 \mathbf{F} \cdot D \cdot \mathbf{G} \\ &= 8W^2(2L+1) |R_L|^2 [(\mathbf{F} \cdot \mathbf{G}) \\ &\quad - Q^{-2}(\mathbf{F} \cdot \mathbf{Q})(\mathbf{G} \cdot \mathbf{Q})]. \end{aligned}$$

In particular

$$\begin{aligned} \sum_M (\mathbf{q}; \mathbf{q}) &= \sum_M (\mathbf{P}; \mathbf{P}) = -\sum_M \text{Re}(\mathbf{P}; \mathbf{q}) \\ &= 8W^2(2L+1) |R_L|^2 P^2 q^2 (1-\mu^2) Q^{-2}. \end{aligned}$$

APPENDIX II

Evaluation of $|R_L|^2$

$|R_L|^2$, where R_L is given by Eq. (A-1), must be evaluated. As is consistent with our previous approximations, correction terms in αZ are to be neglected. If $Q \neq W$ (i.e., if Q is not approximately equal to W), the exponential then simply serves as a convergence factor, i.e.,

$$R_L(Q \neq W) \approx \text{Lim}(Z \rightarrow 0) R_L,$$

where the limiting process must be performed after the integration. This latter expression is equivalent to

$$\text{Lim}(Z \rightarrow 0) \int_0^\infty j_L(Qx) h_L^{(1)}(W'x) x^2 dx,$$

where $W' = W + im\alpha Zx$. In this form the integral can readily be performed, and we find

$$|R_L(Q \neq W)|^2 \approx (1/W^2)(Q^2/W^2)^L (Q^2 - W^2)^{-2}.$$

This approximation is obviously not valid for $Q = W$. Since the integrand is bounded, the divergence at $Q = W$ must be due to the infinite range of integration. It is then sufficient for our purposes, in the neighborhood of $Q = W$, to replace j_L and $h_L^{(1)}$ by their asymptotic forms, in which case the integration is trivial. Neglecting correction terms in αZ , and replacing Q by W in some terms, we find

$$|R_L(Q \approx W)|^2 \approx (1/W^2)[(Q^2 - W^2)^2 + (2mW\alpha Z)^2]^{-1}.$$

A form which is applicable over the entire range is then

$$|R_L|^2 \approx (1/W^2)(Q^2/W^2)^L [(Q^2 - W^2)^2 + (2mW\alpha Z)^2]^{-1}.$$

It is to be noted that the radial integral R_L arises in internal conversion in the Born approximation with Q replaced by P' , the momentum of the ejected electron. Unlike Q , the momentum P' has a definite value, namely,

$$P' = [(W+m)^2 - m^2]^{1/2} \neq W.$$

The situation corresponding to $Q = W$ therefore does not exist in internal conversion. The physical meaning of this difference is that in the internal Compton process, as opposed to internal conversion, the virtual photon can conserve energy even in the Born approximation.

APPENDIX III

The decay factor $\exp(-\Delta E t_0)$ is justified by the realization that the amplitudes of the states that we are interested in, namely, those which arise via an internal Compton transition, satisfy a set of differential equations in which they are coupled to the initial state but not to one another. The specification of the time dependence of the amplitude of the initial state then determines the time dependence of all of the other amplitudes. The use of the decay factor could have been avoided in a number of ways. One method would be the usual one of analyzing the time dependence of the initial state amplitude only for infinitesimal times after $t=0$. Another method would be the determination of the energy shift of the initial state by the use of Feynman diagrams in which the initial and final states involve the nucleus in its excited state and the K electron in its ground state and the intermediate states are those which arise in an internal Compton transition. The negative imaginary part of the energy shift, which is one-half of the initial transition rate, is found by considering those internal Compton intermediate states in which energy is conserved. There are four possible Feynman diagrams; two of the diagrams consist of one of the diagrams of Fig. 1 followed by its mirror image and two consist of one of the diagrams of Fig. 1 followed by the mirror image of the other.

APPENDIX IV

Evaluation of M_2

The expression for M_2 involves the integral

$$\int \exp(-m\alpha Z x_7 - i\mathbf{q} \cdot \mathbf{x}_7 - i\mathbf{p} \cdot \mathbf{x}_7 + i\mathbf{p} \cdot \mathbf{x}_5) (\mathbf{p} - m)^{-1} d^3 \mathbf{x}_7 d^3 \mathbf{p}.$$

Unlike the situation for M_1 , integration over \mathbf{x}_7 does not lead to a δ function, so that integration over \mathbf{p} cannot readily be performed. However, it is permissible at the outset to replace the \mathbf{p} which appears in \mathbf{p} by $(-\mathbf{q})$. This would be exact were it not for the factor $\exp(-m\alpha Z x_7)$. Integration over \mathbf{p} and \mathbf{x}_7 is then trivial and one arrives at the result given in Eq. (24).

The factor $\exp(-m\alpha Z x_7)$ cannot simply be dropped, for it is ultimately required for convergence. The re-

placement of \mathbf{p} by $(-\mathbf{q})$ in \mathbf{p} corresponds to the neglect of Fourier momentum components of order m , or, equivalently, to the neglect of residues due to the poles of $(\mathbf{p}-m)^{-1}$. (A pole occurs on the real axis only if the real photon has an energy $q \geq 2m$, for if energy is to be

conserved in the intermediate state the electron must jump into a negative energy state.) The error involved in the replacement of \mathbf{p} by $(-\mathbf{q})$ in \mathbf{p} is of order αZ , and the approximation is therefore consistent with previous ones.

Average Neutron Total Cross Sections in the 3- to 12-Mev Region*

NORRIS NERESON AND SPERRY DARDEN†

University of California, Los Alamos Scientific Laboratory, Los Alamos, New Mexico

(Received March 1, 1954)

Measurements of the average neutron total cross sections of N, F, Mg, P, Cl, Ti, Mn, Co, Ni, Zn, Se, Br, Mo, Ag, Cd, Sn, Sb, Te, La, Ta, W, Au, Hg, and Tl have been made over the 3- to 12-Mev energy range. The average energy spread of the measurements is approximately 10 percent and the over-all accuracy of the results is ± 10 percent or better. The above data, together with those of a previous experiment, provide information on average cross-section behavior as a function of energy and atomic weight over most of the periodic table.

AVERAGE total cross sections for neutrons have been measured for a set of 24 elements over the 3- to 12-Mev energy region. The present measurements are an extension of a set of previous measurements made for 13 elements.¹ These earlier measurements showed that neighboring elements exhibit similar patterns in their average cross-section behavior. The aim of the present experiment was to supplement the previous data and to establish cross-section trends over the entire periodic table. Therefore, most of the elements were selected with the above objective in view; however, certain elements were chosen as a result of specific requests for total cross-section information.

The experimental arrangement for the present measurements was the same as that used in the previous measurements except for an improvement in the sample and detector geometry. In the present case, the distance from the sample to the detector was increased to 18 inches as compared to 11 inches in the earlier arrangement. All of the scattering samples were 1 inch in diameter and their length was chosen so as to give a neutron transmission of approximately 0.5. During the course of the work, the neutron source for the experiment was changed from one reactor to another reactor. The data from 6 to 13 Mev were obtained by using the Los Alamos fast reactor as previously described, while the 3- to 6-Mev data were acquired by using a U^{235} converter² placed in a hole which goes

through the center of the Los Alamos water boiler. The neutron spectrum obtained from these two sources is the same over the energy region utilized for this experiment, i.e., above 3 Mev.

The results presented here retain the same characteristics as the previous measurements, i.e., the average energy spread is about 10 percent of the measured energy, and the over-all accuracy is at least ± 10 percent over the 3- to 12-Mev energy range. Above 12 Mev the present data are subject to considerable error and the more accurate 14.1-Mev point obtained by Coon and others³ has been weighted accordingly in determining the curve over the 12- to 14-Mev region. As previously, a smooth curve has been drawn through the data points and small fluctuations which are not well resolved by the experiment have been averaged over the curve. A curve has not been drawn where better-resolved data already exist. No corrections have been made on the measured cross sections for the effect of neutrons scattered into the detector by the sample. The geometry is such that this correction is probably less than 1.5 percent at 12 Mev.

The results obtained are shown in Figs. 1, 2, and 3 where the average neutron total cross section, σ_t , is plotted as a function of the neutron energy, E_n . In Fig. 1 the two sets of nitrogen data do not agree well over certain energy regions. The measurement employing melamine and polyethylene is probably

thickness of 0.01 inch and a diameter slightly less than 1 inch. This series of disks were sealed in an aluminum tube 3 feet long and 1 inch diameter and placed at the center of the reactor where the average thermal neutron flux is about 10^{12} . At a neutron energy of 3 Mev, this converter produced a collimated neutron flux at the wall of the reactor (77 inches distant from the converter) of 9×10^6 neutrons $\text{cm}^{-2} \text{sec}^{-1} \text{Mev}^{-1}$. The above figures are for a water boiler power of 25 kilowatts.

³ Coon, Graves, and Barschall, *Phys. Rev.* **88**, 562 (1952).

* This work was performed under the auspices of the U. S. Atomic Energy Commission.

† Present address: Department of Physics, University of Wisconsin, Madison, Wisconsin.

¹ N. Nereson and S. Darden, *Phys. Rev.* **89**, 775 (1953).

² This converter was made by L. D. P. King of this laboratory and consisted of an assembly of 120 U^{235} disks each having a